ELSEVIER

Biophysical Chemistry 103 (2003) 139–156

Biophysical Chemistry

www.elsevier.com/locate/bpc

Molecular dynamics investigation of an antibody binding site by the fluorescence–photochrome method

Oren Chen, Robert Glaser, Gertz I. Likhtenshtein*

Department of Chemistry, Ben-Gurion University of the Negev, Beer-Sheva 84104, Israel

Received 2 June 2002; received in revised form 22 August 2002; accepted 26 August 2002

Abstract

A combined fluorescence–photochrome approach was used for investigation of the molecular dynamics antiDNP antibody binding site and its cavity. A 4-(*N*-2,4-dinitrophenylamino)-4′-(*N*,*N*′-dimethylamino)stilbene (StDNP) fluorescence DNP analog was incorporated into the antibody binding site. This was followed by measurements of fluorescence and photochrome parameters such as the StDNP excitation and emission spectra, fluorescence lifetime, steady-state and time-resolved fluorescence polarization, kinetics of *trans–cis* and *cis–trans* photoisomerization, and fluorescence quenching by nitroxide radicals freely diffused in solution. In parallel, computational modeling studies on the location and dynamics of DNP/TEMPO spin-label (Ns*l*DNP) and StDNP guests within a model of the binding site were performed. When all the experimental evidence is considered (including data from the antibody X-ray study), one can conclude that wobbling of the Trp 91 L/Trp 96 H binding-site•bound-hapten moiety (StDNP), can be responsible for the label's nanosecond dynamics monitored by fluorescence polarization techniques. A similar conclusion may be reached as a result of data analysis on Ns*l*DNP mobility within the antibody binding site. The mobility of Trp 91 L and Trp 96 H moieties provides the induced fit needed for effective stacking and release of the DNP epitope. Analysis of the above-mentioned data allows one to explore the mechanism of the probe's movement within the binding site and enables one to discuss the local dynamics of the binding site region. The combined fluorescence–photochrome approach can be used for investigation of local medium molecular dynamics in the immediate vicinity of specific sites of proteins and nucleic acids, as well as for other biologically important structures and synthetic analogues.

Keywords: 2,4-Dinitrophenyl; Antibody; Binding-site; Fluorescence–photochrome; Molecular-dynamics; Molecular probes

1. Introduction

The basis of much of our present conception of intermolecular protein dynamics is based on hypotheses put forward in the 1950s and 1960s [1–3]. Later in the 1960s and 1970s, considerable indirect evidence was obtained in favor of mobility of proteins. Subsequently, more direct approaches were intensively developed for the investigation of protein dynamics. Their distinctive features were the application of physical methods (such as NMR, fluorescence, differential scanning calorimetry, X-

*Corresponding author. Tel.: +972-86472187; fax: +972-86472943.

E-mail address: gertz@bgumail.bgu.ac.il (G.I. Likhtenshtein).

0301-4622/03/$ - see front matter © 2002 Elsevier Science B.V. All rights reserved.
PII: S0301-4622(02)00252-1

ray and neutron scattering) towards the study of this important phenomenon. The most significant progress in this area was achieved by the use of spin, fluorescence and Mössbauer labeling methods [4–9].

Considerable evidence indicates that 'hinge-bending' (of blocks, domains) in protein dynamics plays a key role in protein function; in catalysis by enzymes; and in particular, for electron transfer ([6–15]; and references therein). It was suggested that the processes of complex formation between antigens and antibodies, allosteric regulation, mechanical transformation, and conformational transition in the course of enzyme catalysis only proceed due to the ability of protein globules to undergo rapid and reversible changes of conformation.

It has been repeatedly stressed that intramolecular protein mobility is significantly dependent on the molecular dynamics of the surrounding medium. These surroundings provide the free volume necessary for movement of protein domains and individual functional groups [6–10,12,14]. The environmental dependence of protein behavior is central to the biological function of macromolecular systems (proteins, in particular). Starting from the early 1960s, increasing evidence has been found linking protein functional activity and stability together with a decisive role for the dynamics of water (and other molecules) surrounding the globular entities.

The various types of immunoglobular internal motion were investigated by almost the complete arsenal of physicochemical methods ([16,17]; and references therein). It was shown that dynamic properties of protein subfragments bearing binding sites provide the ability to form specific stable complexes with a vast array of antigen molecules via the 'induced fit mechanism'. Nevertheless, the dynamic status of binding sites and the medium in the immediate vicinity of immunoglobulin binding sites was not sufficiently investigated.

One of the promising approaches for the molecular dynamics investigation of biologically important or synthesized molecules involves the use stilbene derivatives as probes. The fluorescence and photoisomerization of stilbenes have been extensively investigated for decades, and this topic has been reviewed [18–21]. Stilbene derivatives are relatively easily synthesized, are usually thermally and chemically stable, and possess absorption and fluorescence properties that are convenient for monitoring by relevant optical techniques. It has been shown that stilbenes exhibit fluorescence characteristics that are similar to those of typical membrane and protein fluorescence probes. In addition, the quantitative study of direct and sensitized stilbene photoisomerization opens up new possibilities for measurement of probe rotational and translational diffusion [21–29].

Since the *cis*-stilbene diastereomeric form is not fluorescent at steady-state conditions, rate measurements of decreased emitted fluorescence from the *trans*-form can monitor the *trans–cis* photoisomerization process. The fluorescence–photochrome properties of the probe reflect, in turn, the polarity and molecular dynamics ('microviscosity') of the medium in the probe's vicinity.

The photochrome–fluorescence method is based on monitoring fluorescence parameters and kinet-

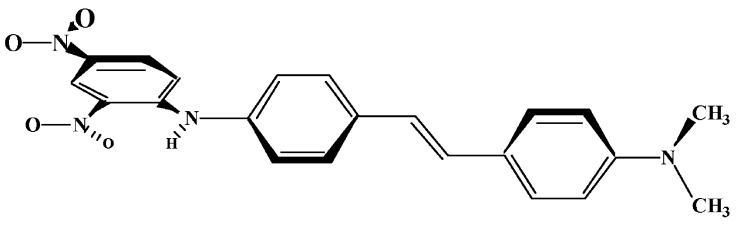

1

ics of *trans–cis* and *cis–trans* photoisomerization of *para*-substituted stilbenes. It was proposed and developed for investigating the molecular dynamics, microviscosity and phase transition in proteins and biomembranes [21–26]. It has been shown that the apparent rate constant of the photoisomerization in viscous media is controlled, in certain cases, by the relaxation rate of the medium [18,19,23,24,28]. Thus, after appropriate calibration, it is possible to estimate the frequency for 180° twists about the stilbene fragment's exited singlet-state single-bond. In addition, stilbene probe mobility can be monitored by the conventional fluorescence polarization technique. Data on photochrome and fluorescence properties of probes, when taken together, make it possible to establish the detailed mechanism of the probe's motion and afford an estimation of the motional parameters.

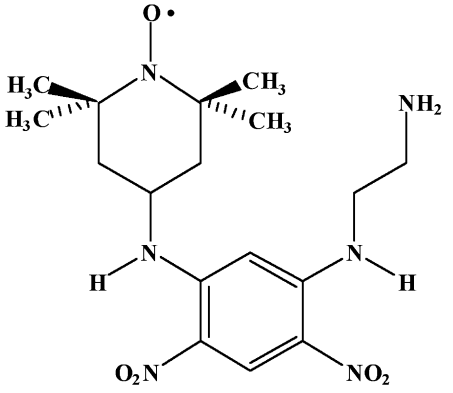

3

An X-ray crystallographically determined structure of an monoclonal AN02 Fab fragment anti-DNP antibody/spin-label hapten derivative complex (**2**, Brookhaven PDB ID 1BAF) has been reported [30]. The structure consisted of a 4-[5-(2-amino-ethylamino)-2,4-dinitrophenylamino]-2,2,6,6-tetramethyl-1-piperidinoxyl radical (**3**, Ns*l*DNP) nitroxide spin-labeled hapten bound within the antibody binding site. The bound TEMPO-type nitroxide spin-label had been used to study nearby residues in the antibody binding site via paramagnetic line broadening in the NMR spectrum [31]. Since the structure of this AN02 Fab fragment antibody/spin-label hapten complex was known, it provided an opportunity for using it as a putative relatively close structural model for the antiDNP antibody in molecular graphics studies to complement the other experimental investigations to be reported in this work.

The basic concept underlying our approach was to first bind a fluorescent–photochrome stilbene label hapten-conjugate (**1**) to the antiDNP antibody binding site. This was followed by monitoring the kinetics of fluorescence, quenching of fluorescence, fluorescence polarization, and *trans–cis* photoisomerization of the label in the binding site compared to the kinetics of these processes for the free state. StDNP photoisomerization can occur via the excited singlet-state (or/and the triplet state which may be created as a result of enhanced intersystem crossing). In any event, the photoisomerization mechanism of the probe's stilbene fragment is not essential for the interpretation of experimental results. To produce the *cis*-form, the stilbene *trans* double-bond must undergo twisting via any of the possible states (excited singlet or triplet). The important point to remember is that the photoisomerization rate is dependent, to a certain extent, on the microviscosity and steric hindrance in the vicinity of the double-bond (Sun and Saltiel [18,19,21,24]; and references therein). According to our estimation (Section 3.1), the StDNP can be considered to be a rigid structure molecule on a nanosecond time-scale. This molecule can be appropriately used as a probe of microenvironment nanosecond dynamics in the antiDNP antibody, since our approach is based on a comparison of the probe's molecular dynamics in solution, and within the antibody binding site, together with direct experimental measurement of above mentioned parameters.

In the present work, we investigated the molecular photoisomerization and dynamics of the stilbene probe 4-(*N*-2,4-dinitrophenylamino)-4′-(*N*,*N*′-dimethylamino)stilbene (StDNP), **1**, in the antiDNP antibody binding site. In parallel, computer assisted molecular graphics modeling of the position of the StDNP hapten (or Ns*l*DNP spin-probe) in the AN02 Fab fragment model for antiDNP was performed. Barriers for bond-rota-

tion, estimated from computer calculated torsion angle driving studies of bonds in the StDNP hapten (or Ns*l*DNP spin-probe), were made to facilitate interpretation of the antibody-bound probe's experimentally determined mobility parameters. Analysis of the above-mentioned data allows one to explore the mechanism of the probe's movement within the binding site. These studies probe the 'microviscosity' of the medium in the immediate vicinity of the binding site, and enables one to discuss the local dynamics of the binding site region.

2. Methods

2.1. Preparation of reagents

4-(*N*-2,4-Dinitrophenylamino)-4′-(*N*,*N*′-dimethylamino)stilbene label (StDNP), 1, was prepared from a saturated abs. ethanolic solution of *trans*-4-dimethylamino-4′-aminostilbene [25,26] added to an equimolar saturated abs. ethanolic solution of 2,4-dinitrochloro-benzene (Aldrich) under magnetic stirring to yield an initially clear reaction mixture which was left overnight. The resulting precipitated brown crystalline solid was collected by vacuum filtration, and washed with water and petroleum ether (60–80 °C). The crude product was recrystallized from chlorobenzene, and then dried in a vacuum oven. Elemental and ^{1}H NMR (200 MHz, $CDCl_3$) analyses of StDNP (**1**) were in complete accord with its proposed structure.

2.2. Fluorescence–photochrome technique

An Aminco-Bowman SLM 4800 GREG-MM multi-frequency phase-modulation spectrofluorimeter upgraded by ISS was used for fluorescence intensity, kinetics of reversible *trans–cis* photoisomerization, and fluorescence polarization measurements of the free StDNP label (and also of the antiDNP–StDNP complex). The absorption spectrum of the samples was measured on a Packard HP 89532A UV–visible spectrophotometer. Analysis of the experimental data was performed using the KALEIDAGRAPH 3.0.5 (Abelbeck Software) program.

Fluorescence measurements of the free StDNP label were performed in a solvent mixture composed of glycerol (50%), buffer phosphate saline (40%), which contained NaCl (137 mM), Na_2HPO_4 (4.3 mM), KCl (2.7 mM), KH_2PO_4 (1.2 mM), and DMSO (10%). This solvent composition (designated as *solvent mixture-A*) was found to afford the conditions for optimum solubility of the components on one hand, and for optimum intensities of fluorescence, on the other. The average fluorescence polarization parameters and *trans–cis* isomerization rate constant of StDNP were measured at a constant 2 μM label concentration, each polarization value is an average of at least 10 measurements (of the same sample).

Fluorescence emission of StDNP was recorded at $\lambda_{em} = 438$ nm after excitation near its absorption maximum at $\lambda_{ex} = 350$ nm (a 16-nm slit-width for excitation and emission was typically used).

The reversible *trans–cis* reaction kinetics of the free StDNP label was measured by continuously irradiating the sample at $\lambda_{ex} = 350$ nm for a period of 500 s, followed by an emission measurement at $\lambda_{em} = 438$ nm. For measurement of *cis–trans* photoisomerization, the sample was then irradiated at a shorter wavelength ($\lambda_{ex} = 300$ nm, where mainly the *cis*-diastereomer absorbs) for an additional 500 s, again followed by an emission measurement at $\lambda_{em} = 438$ nm.

The rate constant value of change in StDNP fluorescence emission intensity (I) as a function of time (t) was calculated according to Eq. (1):

$$\ln\left(1 - \Delta I_t / \Delta I_\infty\right) = -k_{iso} t \quad (1)$$

where t is the time, k_{iso} is the first order rate constant; $\Delta I_t = I_0 - I_t$; $\Delta I_\infty = I_0 - I_{t_{max}}$; I_0 is the fluorescence intensity at time $t = 0$; I_t is the fluorescence intensity at time t; and $I_{t_{max}}$ is the fluorescence intensity at $t = t_{max}$. Since different concentrations of antibody afford different optical densities for each sample, a correction was made according to Eq. (2):

$$k_{iso\ (corrected)} = 10^D k_{iso\ (measured)} \quad (2)$$

where $D = X[AD]/[AX]$, while D and X are the optical densities for the samples of the antibody at concentrations $[AD]$ and $[AX]$, respectively.

2.3. Fluorescent lifetime (τ_f), and average rotational correlation time (τ_c) measurement

Variable–frequency phase and modulation data were measured with an ISS K2 Multifrequency Cross-correlation Phase and Modulation Fluorimeter, using a dry milk scattering solution. Excitation was performed using a 300 W arc xenon lamp with the excitation monochromator set for a 16-nm bandwidth. Emission bands were selected using cutoff filters ($\lambda_{em} > 430$ nm). The modulation frequency was continuously varied from 10–20 to 200–250 MHz. The number of modulation frequencies used was generally 25. Decay data were fitted using software provided by ISS Inc. The data fit was based upon the sum of exponential components, characterized by the lifetime τ and the fractional intensity, f. Frequency-independent standard errors for phase and modulation were assumed to be 0.5° and 0.01, respectively. Spectral data were obtained at a temperature of 25 ± 0.5° using a circulating water bath. Samples were excited at 350 nm. Values are the average of two or three measurements. An ISS-GREG-90 phase-modulation fluorimeter with modulation frequencies between 20 and 190 MHz was employed for the lifetime measurements in some of the experiments.

Polyclonal antiDNP antibodies (Sigma) developed in rabbit were used for measuring fluorescence lifetime, rotational correlation time, polarization and isomerization rate constant of the antiDNP–StDNP complex. A monoclonal antiDNP antibody (Biomeda, USA) developed in goat were used for measuring the fluorescence emission and excitation spectra, and fluorescence lifetime of the antiDNP–StDNP complex in the presence of an increasing concentration of 4-hydroxy-TEMPO (Sigma).

2.4. Computation

Computer simulation was performed using the following software: MACSPARTAN PLUS 1.2.1 (Wavefunction, Irvine, CA), PCMODEL 5.03 Macintosh version (Serena Software, Bloomington, IN), BALL-AND-STICK 3.7 (N. Mueller, Johannes Kepler Universität, Linz), and MACMIMIC 3.0 (InStar Software, Lund, Sweden). The X-ray crystallographically determined structure of the monoclonal AN02 Fab fragment antiDNP antibody-bound nitroxide spin-labeled DNP-hapten complex (**2**), {antiDNP/4-[5-(2-amino-ethylamino)-2,4-dinitrophenylamino]-2,2,6,6-tetramethyl-1-piperidinoxyl radical (**3**, Ns*l*DNP) [30]} was retrieved from the Brookhaven Protein Data Bank (Brookhaven PDB ID 1BAF).

3. Results and discussion

3.1. Computer assisted molecular modeling

A molecular mechanics stochastic search of energetically accessible *trans*-StDNP conformations was undertaken using the GMMX subprogram of PCModel. These conformations were then used as input structures for ab initio geometry optimization calculations (RHF/3-21G* basis set). The StDNP ab initio global minimum molecular model used in this study has a non-planar conformation. The two aromatic rings of the *trans*-stilbene moiety are bent into a propeller-like chiral conformation, each stilbene ring is twisted 23 ± 4° with the same helicity to afford a pseudo-C_2 axis through the olefinic hub. The dinitrophenylanaline trigonal nitrogen is coplanar with the dinitrophenyl ring, and the adjacent stilbenyl aromatic ring is orthogonal to the dinitrophenylanaline plane. The structure depicted for 1 is a CHEM3D PRO 5.0 (CambridgeSoft, Cambridge, MA) generated iconic 2D projection of the StDNP-label computer calculated 3D molecular model.

The X-ray crystallographically determined structure of 4-[5-(2-amino-ethylamino)-2,4-dinitrophenylamino]-2,2,6,6-tetramethyl-1-piperidinoxyl radical (**3**, Ns*l*DNP) hapten derivative bound within the AN02 Fab fragment model for the antiDNP antibody was used as a starting point for molecular graphics modeling studies [30,31]. The Ns*l*DNP nitroxide spin-labeled hapten is held between the pyrrole moieties of two parallel tryptophanyl planes separated by 7.3 Å in the X-ray structure. The two-tryptophanyl moieties are located in different chains of the antibody (the V_H and V_L variable domains form the antigen binding site). The normal from the DNP ring to the plane of

one of the tryptophanyl rings is 3.5 Å, while that to the other tryptophanyl ring-plane is 3.8 Å. The tryptophanyl pyrrole nitrogen atoms point in the same direction [5.1° N–H···N′–H′ torsion angle], but different tryptophanyl ring faces point toward the DNP-ring. The binding site is located in a cleft between the V_H and V_L domains whose narrowest region has a 98° angle between two lines originating at the center of the DNP ring and extending outwards into space. The DNP ring of StDNP-label (**1**) was superimposed on upon the DNP ring of Ns*l*DNP (**3**), and then the derivatized hapten Ns*l*DNP was removed. Since the 2,4-nitro disubstitution pattern in **1** is unsymmetrical, there are two potential docking modes. Fig. 1 shows 2D-iconic projections of the 3D model in which the 2- and 4-nitro groups occupy sites 'A' (pointing inwards in the drawing) and 'B' (pointing outwards in the drawing), respectively, while Fig. 2 shows these same groups now residing in the opposing sites. The steric barrier of neighboring residues surrounding the binding site has been depicted as a folded sheet in both figures. The iconically drawn steric barrier was constructed by drawing 10 Å lines originating from the 2,4-dinitrophenyl ring center outward through nearest atoms in surrounding residues within the binding-site. For ease of viewing, the lines were then terminated 4.75 Å from their outermost terminus rather than approach the ring center.

Inspection of these illustrations shows that in the AN02 Fab fragment model for antiDNP, there is sufficient room for *trans–cis* stilbene photoisomerization to occur in both binding modes. The StDNP label did not penetrate the folded steric barrier when rotation was performed about the double-bond in both binding mode models. In addition, StDNP single-bonds in both molecular model binding modes were rotated to ascertain potential interactions with the binding site steric barriers. These studies clearly showed that the binding site barriers were far enough away to permit single-bond rotation about the DNP–N, $DNP_{anilinyl}$ N–C_{ipso} (stilbene) bond as well as for the two single-bonds on either side of the stilbenyl double-bond. Torsion angle driving studies were undertaken to estimate rotational barriers about the $C_{DNPipso}$–N and N–$C_{STILBENYLipso}$ bonds using (2,4-dinitro-phenyl)-phenyl-amine as a model compound. Geometry optimization of the model compound gives the same ground state conformation as found for StDNP 1 [synperiplanar −0.9(5)° H–N–$C(1)_{DNPipso}$–$C(2)_{DNPortho}$ mean torsion angle (angle ψ), and orthogonal 90.2(5)° H–N–$C(1')_{PHENYLipso}$–$C(2')_{PHENYLortho}$ mean torsion angle (angle ϕ)]. In these driving studies of bonds on either side of the N-atom, each torsion angle was separately constrained after rotation about the particular C–N bond by a 10° increment, while the second C–N bond remained unfettered (free). The resulting input then underwent ab initio RHF/3-21G* geometry optimization. As the constrained C–N torsion angle value was 'driven' by 10° increments, the resulting set of computed energies went through a maxima and then decreased. This maxima provided an estimated $\Delta H^{\ddagger}$ C–$N_{ANILINYL}$ bond rotation barrier for use in correlation time (τ) calculations discussed below.

A 16.7 kcal mol^{-1} barrier was observed for the N–$C(1)_{DNPipso}$ bond [ψ = −100° (constrained), ϕ = 7.5°]. For the N–$C(1')_{PHENYLipso}$ bond, a barrier of 5.7 kcal mol^{-1} was found when ψ = 19.6° and ϕ = 0° (constrained)]. In this energy maxima, the nitrogen non-bonded electron pair is delocalized into the phenyl ring. Some degree of electron delocalization still occurs into the DNP ring when ψ = 19.6° (since delocalization is a cosine function of angle ψ), and the 2-nitro oxygen still maintains a hydrogen-bond to the N–*H* [6.8° $N_{ANILINYL}$–H_N···$O_{2\text{-}nitro}$–$N_{2\text{-}nitro}$].

Values of the estimated correlation time τ for intramolecular rotation about the C–$N_{ANILINYL}$ bonds in the stilbene and nitroxide probes can be calculated using the Eyring equation:

$$\tau^{-1} = (kT/h)\exp(\Delta S^{\ddagger}/R)\exp(-\Delta H^{\ddagger}/RT) = \tau_0 \exp(-\Delta H^{\ddagger}/RT)$$

where $\Delta S^{\ddagger}$ and $\Delta H^{\ddagger}$ are the respective entropy and calculated enthalpy of activation. According to Benson [32] the entropy for the intramolecular free rotation of bulky radicals, ΔS_R, is approximately 8.5 cal $mole^{-1}$ K^{-1}. Taking this value as the entropy activation for free 'barrierless' bond-rotation and $kT/h = 6 \times 10^{12}$ s^{-1}, one can estimate the bond-rotation correlation time τ′ to be

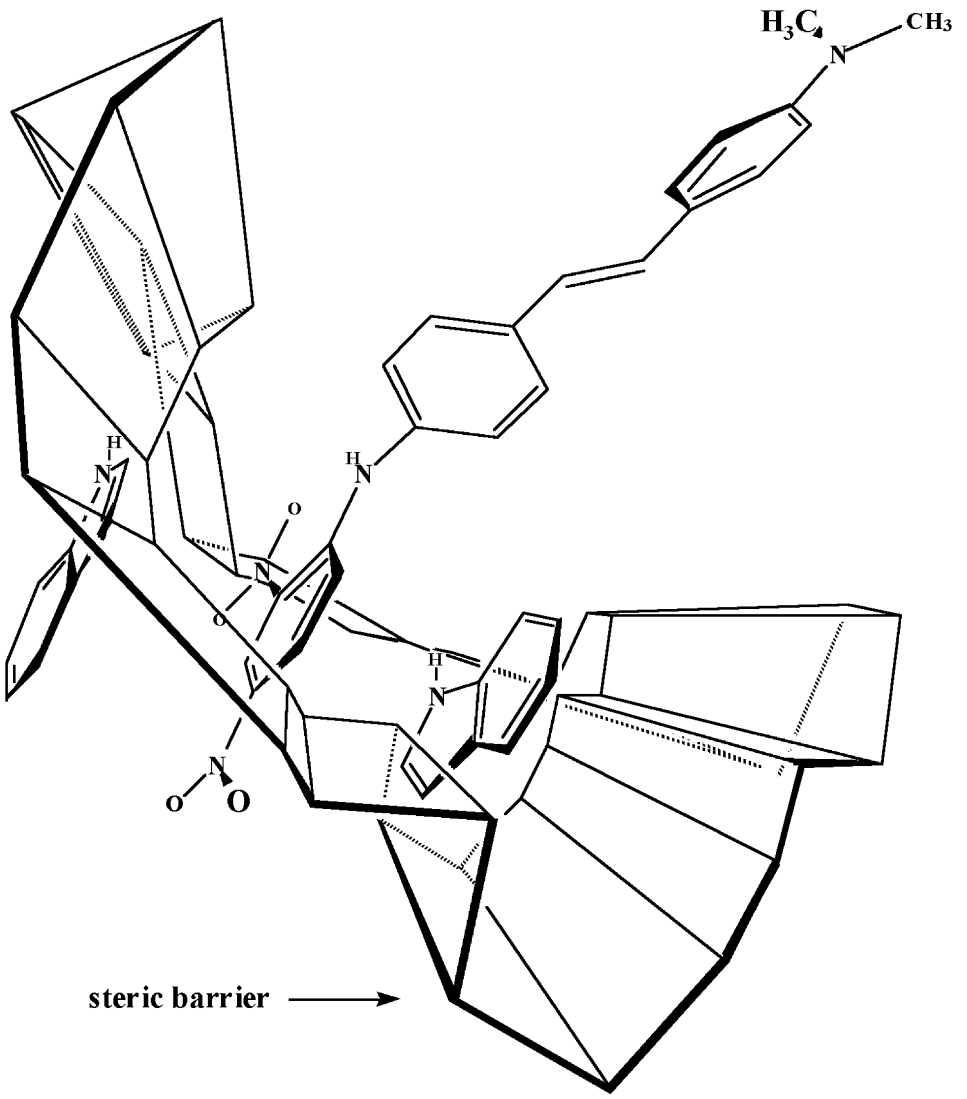

Fig. 1. Iconic drawing of mode 1 binding of StDNP (**1**) in antiDNP antibody binding site viewed down the cleft canyon.

$\sim 1.5\times10^{-12}$ $\exp(\Delta H^{\ddagger}/RT)$ s (τ' is the time for a rotation of one radian).

Using the calculated $+5.7$ kcal mol^{-1} $C_{STILBENYL\,ipso}$–N bond rotation barrier ($E=\Delta H^{\ddagger}$) and a 1.5×10^{-12} s preexponential factor (τ'_0), the N–C(1′)$_{PHENYL\,ipso}$ bond rotational correlation time (τ'_{C-N}) at 300 K (vacuum) may be estimated to be only 19 ns (where $\tau'_{C-N}=\tau'_0 e^{E/RT}$). Using the $+16.7$ kcal mol^{-1} value for the barrier about the adjacent N–C(1′)$_{DNP\,ipso}$ bond, a τ'_{C-N} value of 1.5 s was now estimated.

In a similar manner, (2,4-dinitro-phenyl)-*i*-propyl-amine was utilized as a model compound for Ns*l*DNP, the spin-label nitroxide radical **3** (the C_{METHYL}–H···H–C'_{METHYL} torsion angle was constrained to be 0° to approximate the $C_{METHYLENE}$–$C_{QUATERNARY}$ – $C'_{QUATERNARY}$ – $C'_{METHYLENE}$ arrangement within the piperidinyl ring of Ns*l*DNP.

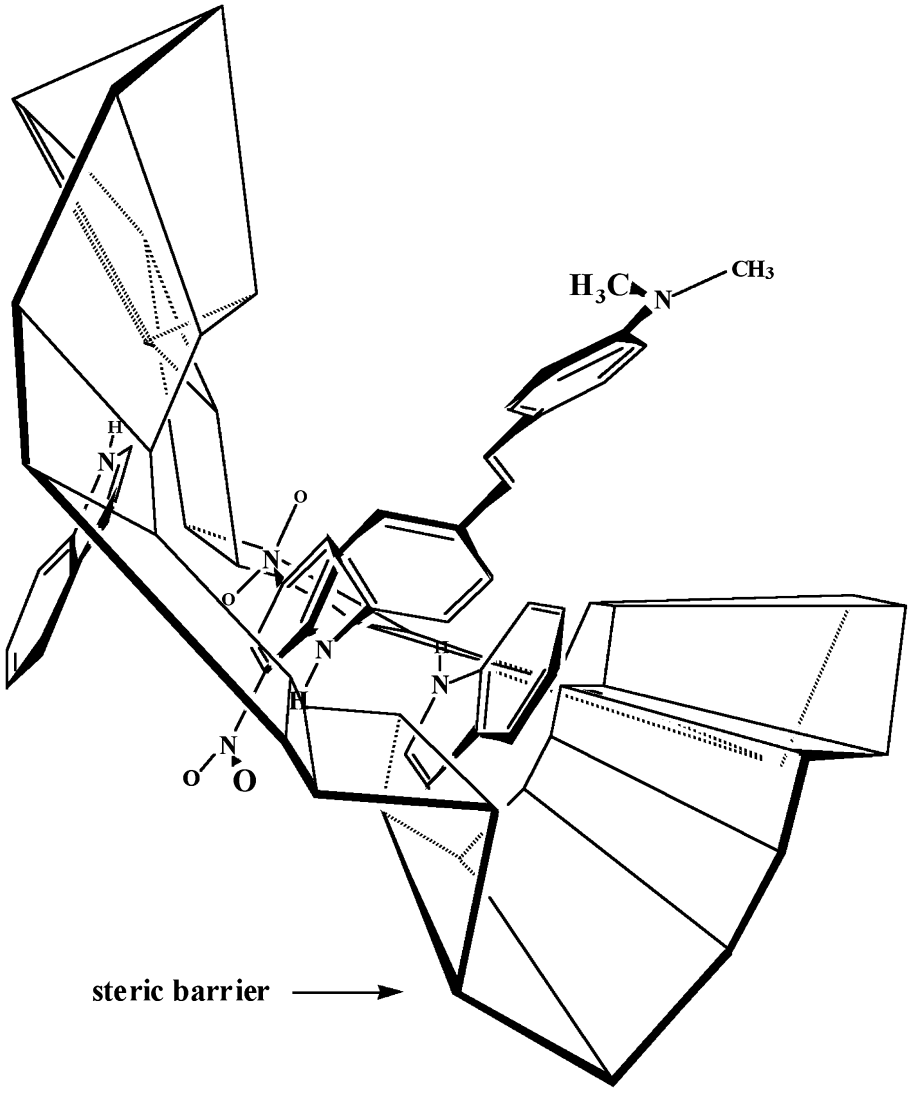

Fig. 2. Iconic drawing of mode 2 binding of StDNP (**1**) in antiDNP antibody binding site viewed down the cleft canyon.

Geometry optimization of the model compound gives the same ground state conformation as found for the Ns*l*DNP nitroxide spin-label [synperiplanar 0.6(1)° H–N–C(1)$_{\mathrm{DNP}ipso}$–C(2)$_{\mathrm{DNP}ortho}$ mean torsion angle (angle ψ), and anticlinal $-138(4)°$ H–C_{METHINE}–N–H mean torsion angle (angle ϕ')]. In the driving study, a steric barrier of 9.6 kcal mol^{-1} about the N–$C_{i\mathrm{PROPYL}methine}$ bond was found when $\psi = 0°$ and $\phi' = \pm 60°$(constrained)]. From this, the bond–rotational correlation time was estimated to be $\tau_{\mathrm{C-N}} = 15$ μs.

Trans–cis photoisomerization quenchers (e.g. the 4-hydroxy-TEMPO nitroxide probe) are expected to suffer reduced accessibility to the stilbenyl double-bond when the label is held in the antibody binding site vs. the free state. This should lead to lower encounter probabilities between these quenching molecules and the bound StDNP label.

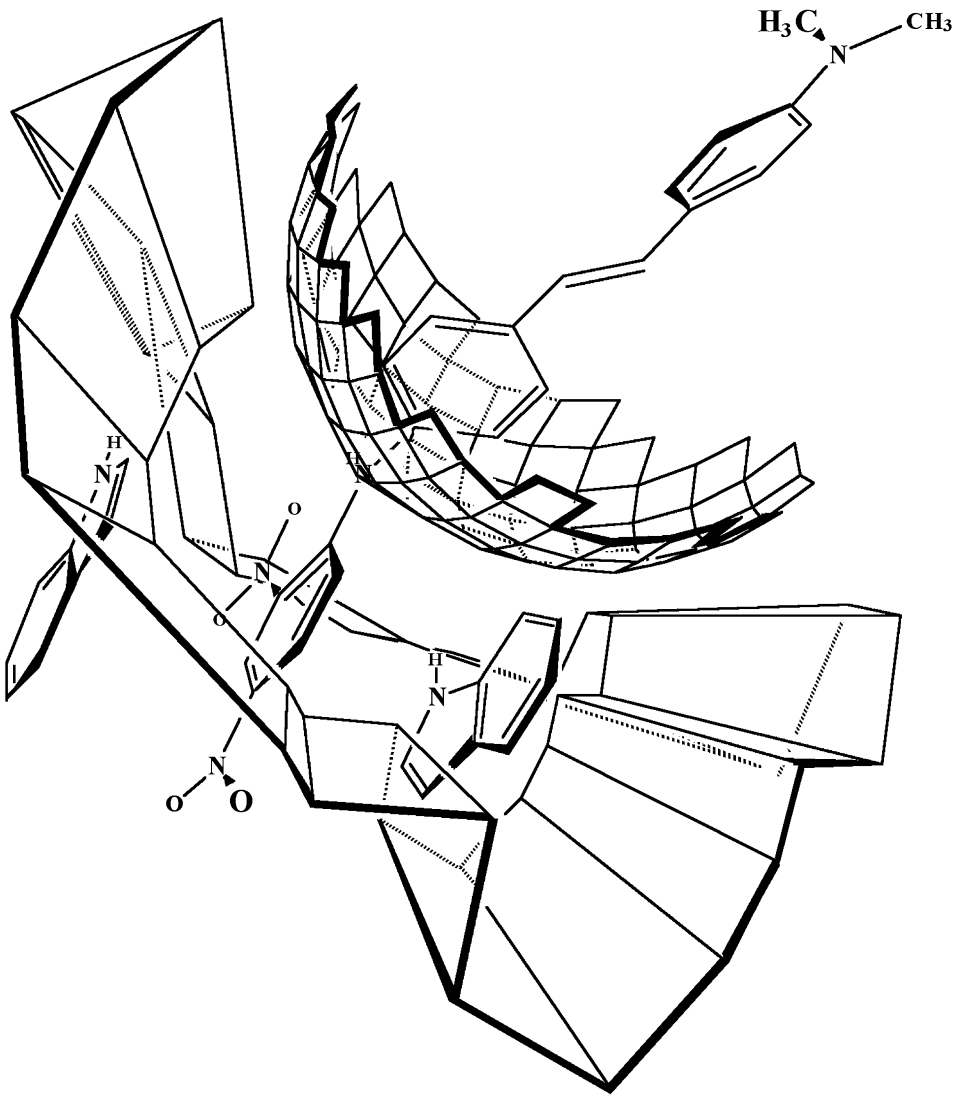

Fig. 3. Iconic drawing of inaccessible surface area on partial sphere drawn with a 1.0 Å radius from double-bond center of mode 1 bound StDNP (**1**) in antiDNP antibody binding site.

A 5.0 Å sphere was circumscribed around the center of the stilbenyl double-bond in both the mode 1 and 2 binding models. Lines were then drawn from the sphere center to each of the outer vertices of the iconic folded sheet binding site barrier. The intersection of these lines with the sphere surface formed an irregular region on the spherical surface. Areas of 85 and 97 $Å^2$ for this region in the respective mode 1 and 2 binding models were estimated by drawing a grid upon the partial sphere's curved surface (e.g. Fig. 3). The fraction consisting of non-accessible surface area/total surface area of sphere can be considered to be a *geometric steric factor* (g_X) effecting quencher encounters with the antibody bound StDNP (**1**) molecule.

Parameter g_X is the ratio of the reaction locus area in particle X relative to the particle's total

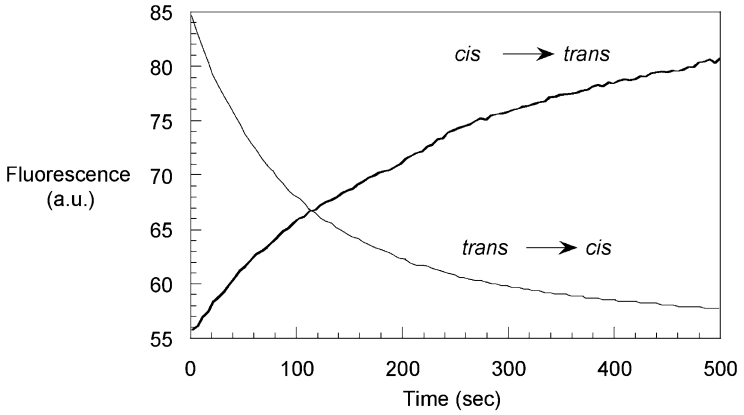

Fig. 4. *Trans–cis* and *cis–trans* photoisomerization of the StDNP label (2 μM) in solution of glycerol (50%), PBS buffer (40%), DMSO (10%). Experimental conditions: excitation 350 nm, emission 438 nm (*trans–cis*), and excitation 300 nm emission 438 nm (*cis–trans*) 25 °C.

area. As shown in Ref. [33], it is necessary to take a 'cage effect' into consideration when under diffusion controlled conditions. This 'cage effect' relates to the possibility of the secondary encounters of particles within the liquid cage. According to the theory, parameter, the *apparent geometric factor* (g_{app}) for encounters between two particles A and B equals $(g_A g_B)^{1/2}$. If one of the particles B is a small molecule while the second one, B, is a protein, then $g_B = 1$ and $g_{app} = g_A^{1/2}$.

Parameter g_X was estimated to be 0.27 [$g_X = 85$ Å^2/314 Å^2, for mode 1], and 0.31 [$g_X = 97$ Å^2/314 Å^2, for mode 2]. Using a 0.29 $g_{X_{mean}}$ value, and taking into consideration the solvent 'cage effect' for encounters at the diffusion limit, we estimated mean *apparent steric factor* $g_{app} = 0.54$ (where $g_{app} = g_X^{1/2}$) for mode 1 and 2 binding models. Based on this, the proximate 'degree of quenching' $(1/g_{app})$ for bound StDNP (**1**) is expected to be approximately 1.9 times less compared to that experienced by the free (unbound) molecule in solution.

3.2. Unbound StDNP (*1*) in solvent mixture-A

The excitation and emission spectra, and kinetics of reversible *trans–cis* and *cis–trans* photoisomerization of the StDNP probe in solvent mixture-A solution was studied by fluorescence techniques. The kinetics of *trans–cis* and *cis–trans* photoisomerization of the StDNP probe in solution-A are shown in Fig. 4. Apparent rate constant values for *trans–cis* and *cis–trans* photoisomerization were found to be $k(t \rightarrow c) = (9.2 \pm 0.1) \times 10^{-3}$ s^{-1} and $k(c \rightarrow t) = (5.1 \pm 0.1) \times 10^{-3}$ s^{-1}, respectively. Experimental data for fluorescence anisotropy (r), fluorescence lifetime (τ_f) and rotational correlation time (τ_c) for label **1** are presented in Table 1.

Two rotational models were considered to analyze possible StDNP label mobility in a given solution of 6 cP viscosity using the above-mentioned experimental data: (1) isotropic rotation and (2) anisotropic ellipsoidal rotation. An estimation of rotational correlation time (τ_c) was calculated using the Perin equation [Eq. (3)] for the case of isotropic rotation:

$$r = r_0/\left(1 + \left(\tau_f/\tau_c\right)\right) \quad \text{where } \tau_c = \eta V/RT \qquad (3)$$

where r and r_0, are the anisotropy in the mobile and immobilized states, respectively; τ_f, τ_c, η, V, R, T are the fluorescence lifetime, rotational correlation time, bulk viscosity, rotation volume swept out by molecule, gas constant, and absolute temperature, respectively. Based on Eq. (3), and an StDNP total rotation volume of $V = 3883$ Å^3, ($r =$ 9.7 Å, half of the molecule length) gives $\tau_{c\text{-}iso} =$ 5.7 ns ($T = 293$ K).

Correlation time $\tau_c = 0.9$–1.5 ns value was estimated by utilization of theoretical curves for prolate ellipsoids of revolution with an experimental

Table 1
Experimental data on fluorescence anisotropy, fluorescence lifetime, and rotational correlation time for free StDNP label 1 and the antiDNP-bound StDNP label in solution (glycerol 50%, buffer 40%, DMSO 10%, viscosity 6 cp)

	Free StDNP label	AntiDNP–StDNP complex
Immobilized-state fluorescence anisotropy[a]	0.37 ± 0.01	–
Mobile-state fluorescence anisotropy (r)	0.19 ± 0.01	0.26 ± 0.01
Fluorescence lifetime (τ_f), ns	0.92 ± 0.10	1.45 ± 0.15
Rotational correlation time (τ_c), ns	1.10 ± 0.10	4.11 ± 0.41

[a] Likhtenshtein et al. [24].

anisotropy $r = 0.19$ [34] and an StDNP elongation parameter (ratio of long axis/short axis) equal to 4.5. The 4.5 value is in the range of the Weber-type model that was calculated for elongation values 3 and 6. The experimental rotational correlation time for free StDNP [$\tau_{\text{c-exptl(unbound)}}$] was 1.1 ± 0.1 ns (Table 1), which is very close to $\tau_{c\perp}$, and is approximately 6–4 times less than $\tau_{\text{c-}iso}$. Taking in account that the calculated correlation times for rotation about the $N_{DNPamino}$–$C_{STILBENYL}$*ipso* bond and N–$C(1')_{DNP}$*ipso* bond in vacuum are equal 19 ns and 1.5 s correspondently, (Section 3.1), we assume that the measured anisotropy, as well the average rotational correlation time of the unbound probe ($\tau_c = 1.1$ ns), mainly refers to anisotropic rotational motion of the probe as a whole.

3.3. StDNP–antiDNP complex in solvent mixture-A

3.3.1. Experimental results and their comparison with the computational model

Addition of antiDNP to the StDNP solvent mixture-A solution led to a gradual increase in the fluorescence polarization. Plots of the polarization value and the probe *trans–cis* photoisomerization rate constant vs. the StDNP/antiDNP ratio are presented in Fig. 5. Enhancement of the polarization value with concomitant increase in the StDNP/antiDNP concentration ratio demonstrates formation of an StDNP–antiDNP complex. The apparent binding constant to our polyclonal antiDNP antibody, K_d, was roughly estimated from experimental dependencies of polarization on ratio

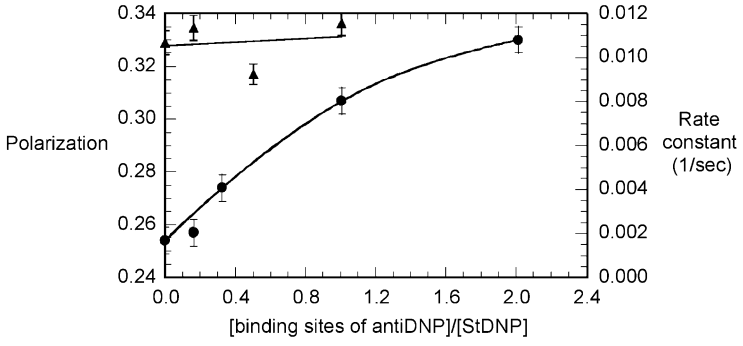

Fig. 5. Fluorescence polarization (circles; left axis) and rate constant of *trans–cis* photoisomerization (triangles; right axis) of StDNP label (2 μM) versus [Polyclonal antiDNP binding sites]/[StDNP] molar ratio. Solution: glycerol (50%), PBS buffer (40%), DMSO (10%), experimental conditions: excitation 350 nm, emission 438 nm, 25 °C.

[binding sites of antiDNP antibody]/[StDNP] using concentration of the binding sites at which the polarization change at addition of the antiDNP antibody is equal to one-half of the maximum change. The K_d value was found to be 1.2 ± 0.2 μM (in a solvent mixture-A solution). This can be compared with K_d values of 0.15 and 0.5 μM previously measured for the binding of Ns*l*DNP and DNPGly to the monoclonal AN02 Fab fragment antiDNP antibody in buffer solution, respectively [31]. The differences in the K_d values may be caused by the differences in the hapten probes structure and solvents property.

Our experiments do not show a marked effect on the photoisomerization rate of the antibody bound StDNP label (Fig. 5). This result is consistent with the molecular model, which indicates free space for *trans–cis* and *cis–trans* photoisomerization of the StDNP stilbene fragment in the StDNP–antiDNP complex (Figs. 1 and 2). Emission and excitation spectra of free and bound StDNP exhibit the same shape. Incorporation of the StDNP label into the DNP antibody binding site was accompanied by a change in the experimental data for fluorescence anisotropy (r), fluorescence lifetime (τ_f) and rotational correlation time (τ_c) (Table 1). For a bound StDNP the anisotropy $r = 0.26$ and $\tau_f = 1.45$ which is markedly higher than that for free label. The experimental value of rotational correlation time $\tau_{c\text{-exptl(bound)}} =$ 4.1 ns was found to be significantly less than the rotational correlation time for the antibody itself [35,36]. Using the fluorescence polarization technique have found that the decay of fluorescence anisotropy in water solution can be described by two rotational correlation times $\tau_{c1} \sim 20$ and $\tau_{c2} =$ 110–140 ns. The τ_{c1} value was ascribed to a twisting of the antibody Fab's fragment along its long axis, and τ_{c2} to the global tumbling of the macromolecule. Similar results were obtained by the spin-labeling method ([16,17]; and references within). The above-mentioned correlation times should by multiplied by factor 6, since the solvent viscosity was 6 cP under the conditions of our experiment. Therefore, the long axis of the bound probe appears to undergo relatively fast motion within what is an essentially slow rotating macromolecule. According to computational molecular graphics modeling of the StDNP docked in an AN02 Fab fragment model for our antiDNP complex (Figs. 1 and 2), the DNP moiety is fixed in the binding site by two tryptophanyl groups, and rotations about single-bonds are prevented by relatively high energetic barriers (Section 3.2). Although computational modeling allows anisotropic rotation about the StDNP $N_{DNPamino}$–$C_{STILBENYL\textit{ipso}}$ bond in the binding site cavity, a suggestion that the polarization correlation time values are related to this motion has to be ruled out. The reason for this is that the experimental $\tau_c = 4$ ns was found to be markedly less than the $\tau_c = 19$ ns value theoretically estimated for vacuum (Section 3.2). In other words, the StDNP label in the antiDNP binding site behaves as a rigid probe.

Taking in consideration all the above-mentioned experimental and computational data, we can conclude that the stilbene probe anisotropic rotation in the nanosecond temporal region reflects the local intramolecular dynamics of the antiDNP antibody binding site. This conclusion was independently confirmed by a reanalysis of the ESR spectrum of the nitroxide spin label DNP derivative (Ns*l*DNP) incorporated in the AN02 Fab fragment antiDNP antibody in buffer solution (using data from Ref. [31]). The spectrum was used as a basis for the estimation of the rotational correlation time τ_c for the probe's nitroxide moiety. Eq. (4) was used for the τ_c estimation:

$$\tau_c = a\left(1 - A_{ZZ}/A_{ZZ0}\right)^b \tag{4}$$

with values of $a = 5.4 \times 10^{-10}$ s and $b = -1.36$ for isotropic Brownian diffusion; and $a = 2.6 \times 10^{-10}$ s and $b = -1.38$ for anisotropic Brownian diffusion [8,9,37,38], and the $A_{ZZ} = 58$ G experimental value of hyperfine splitting taken from the ESR spectrum of the Ns*l*DNP–antiDNP complex in Ref. [31]. The hyperfine splitting values for completely immobilized spin labels attached to proteins in aqueous solution were found to be $A_{ZZ0} = 73 \pm 1$ G over a wide range of temperatures (140–250 K), based on high resolution 2 mm ESR spectroscopy (Krinichnyi, [39–41]). Using such a set of parameters, Eq. (4) affords estimated values for $\tau_c =$ 4.4 and 2.1 ns for the isotropic and anisotropic rotations, respectively.

Both values of the label mobility correlation time are markedly less than the rotational correlation times for rotation of the antibody molecular rotation and the Fabs fragment wobbling but are significantly higher than that for Ns*l*DNP in aqueous solution (0.1 ns) [8,9]. According to our computational modeling the intramolecular isomerization about N–$C_{iPROPYLmethine}$ bond is sterically hindered ($\tau_c = 15$ μs) and the probe DNP moiety is tightly squeezed by two tryptophan groups. This suggests that the nanosecond temporal regime observed for nitroxide anisotropic rotation within the antibody active site is most probably related to local intramolecular dynamics of the antibody in the vicinity of the binding site.

The nitroxide moiety can be involved in two independent dynamic processes: a tumbling of the macromolecule as a whole (or its large fragments) having a correlation time τ_{Cab}, or a rapid wobbling (with a particular angular displacement) of the nitroxide moiety having a correlation time $\tau_\omega < 10^{-10}$ s. The applicability of each model vis-a-vis Anglister et al. [31] to the Ns*l*DNP antibody spin-label experimental data was then considered using a theory developed by Dudich et al. [42]. Taking into consideration the Ns*l*DNP–antiDNP antibody ESR spectrum superfine splitting (58 Gs) and the Fab fragment's $\tau'_{Cab} = 20$ ns experimentally reported [31] values, we can calculate a fast wobbling with a approximately 50° angular displacement. However, it must be recalled that our direct 4 ns measurement of the stilbene probe's correlation time unequivocally indicates that the stilbene fragment (whose size is similar to that of the nitroxide) is involved in high amplitude motion in the nanosecond temporal range. This finding is strong evidence that the tandem Trp 91 L, Trp 96 H, DNP and nitroxide moieties undergo restricted anisotropic twisting with an approximately 2–4 ns correlation time.

Insight into the viscosity in the area the stilbenyl double-bond (located approximately 5 Å away from the DNP fragment squeezed within the confines of the antiDNP binding site) was obtained from the StDNP isomerization data. It has been shown before that the apparent rate constant of photoisomerization in viscous media is controlled, in certain cases, by the particular relaxation rate of the medium [18,19,21,23,24,28]. Specifically, the temperature dependence of the apparent rate constants of *trans–cis* isomerization (k_{iso}) for 4-dimethylamino-4′-aminostilbene in glycerol indicates the existence of two temperature regimes. The apparent rate constant k_{iso} is temperature dependent in the lower temperature regime (11–42 °C), and therefore, it is also viscosity (which constrains the isomerization process) dependent. However, the isomerization rate is temperature independent within the higher temperature regime [24]. The volumes of the stilbene fragments rotated in the excited state and those of nitroxide radicals (e.g. TEMPO) are similar to each other. Thus, the temperature dependent k_{iso} values (and the nitroxide rotational correlation time in the same medium) can be used to estimate the correlation time of the stilbene fragment twisting (rotating) about the single bond in the excited state.

The experimental rate constants of for *trans–cis* photoisomerization (k_{iso}) were found to be similar for the free and antiDNP-bound StDNP label (Fig. 5). According to the above-mentioned experimental data on the temperature dependence of k_{iso}, and therefore, on the 'microviscosity' (nitroxide rotational correlation time τ_c) of the model system, the medium's viscosity does not affect k_{iso} if $\tau_c = 1$ ns [24]. Consequently, the rotational correlation time for the StDNP diaminostilbene fragment is 1 ns. This value is close to the $\tau_c = 1.1$ ns determination based upon the fluorescence polarization for anisotropic rotation of StDNP in the solvent mixture-A solution. Thus, the photoisomerization data show that the microviscosity within the antiDNP binding site cavity (at a distance of approximately 5 Å away from the tryptophanyl binding rings) is close to the viscosity of the bulk medium.

It is necessary to stress, that the above mention experimental data on the stilbene probe fluorescence polarization and photoisomerization were obtained with the use of polyclonal rabbit antiDNP antibodies, and fluorescence quenching by the use of monoclonal goat antiDNP antibodies. The computer assisted molecular modeling utilized the structural model of a mouse monoclonal antibodies, even so, data on the antiDNP antibodies binding sites obtained by physical methods evi-

dence in favor of structural resemblance in the mono- and polyclonal proteins.

Independent information about steric hindrance and microviscosity in the antiDNP antibody binding site cleft was obtained by investigation of StDNP dynamic quenching in free and bound states. Collisional dynamic quenching is described by the Stern–Volmer equation [43]:

$$\tau_{f0}/\tau_f = 1 + K_q[Q] = 1 + k_q\tau_{f0}[Q] \quad (5)$$

where $[Q]$ is the quencher molecule's concentration, τ_{f0} and τ_f are the respective fluorescence lifetimes in the absence and presence of a quencher, k_q is the bimolecular quenching rate constant, and K_q is the Stern–Volmer quenching constant, which is found by plotting τ_{fo}/τ_f vs. $[Q]$.

The Stern–Volmer plot for fluorescence quenching by nitroxide radicals is found to be linear up to a concentration $[R^{\bullet}] = 0.15$ M with Stern–Volmer quenching constants $K_q = 4.6\ M^{-1}$ and $K_{qab} = 3.9\ M^{-1}$ for free and antiDNP bounded StDNP probe respectively (Fig. 6). Taking in account the fluorescence lifetime values for free (0.92 ns) and bound label (1.45 ns) Eq. (5) gives the fluorescence quenching rate constants $k_q = 5.75 \times 10^9\ M^{-1}\,s^{-1}$ and $k_{qab} = 3 \times 10^9\ M^{-1}\,s^{-1}$ for free and bounded StDNP probe accordingly. Thus, from experiment (with the ratio $k_{qab}/k_q = 0.52$) and from molecular graphics ($\xi_{app} = 0.54$), antibody-bound StDNP appears to exhibit approximately 1.9 times less quenching than when it is free in solution (Section 3.1) and 'microviscosity' of the binding site cleft in the area of the fluorescence probe stilbene fragment is close to that of the medium's bulk viscosity.

Computer assisted molecular graphics modeling utilized the monoclonal antibody as a structural model for the polyclonal rabbit antiDNP antibodies used to obtain the above-mentioned experimental data on stilbene probe fluorescence polarization, photisomerization and fluorescence. This is reasonable since data on the antiDNP antibody's binding site obtained by physical methods are in favor of a structural resemblance between mono- and polyclonal proteins. For example, 2,4-dintrophenyl-hapten undergoes similar characteristic spectral shifts in the absorption and circular dichroism spectra when bound specifically to mono-and polyclonal antiDNP antibodies [30,44,45]. Analyses of the NMR spectra of monoclonal murine AN01-12 Fab fragment antibodies bound to the spin-labeled dinitrophenyl-hapten (**3**) show tryptophanyl residues in the vicinity of the hapten [31,45–48]. These findings were confirmed by the X-ray structure of the AN02 Fab fragment/spin-labeled hapten **3** complex which placed the hapten's DNP moiety in a pocket formed by the hypervariable loops so that the DNP ring was sandwiched between the Trp 91 L and Trp 96 H indole rings. The similarity of double difference NMR spectral findings for the complexes between 12 spin-labeled DNP monoclonal AN01-12 Fab fragment antibodies with **3** indicates a structural similarity

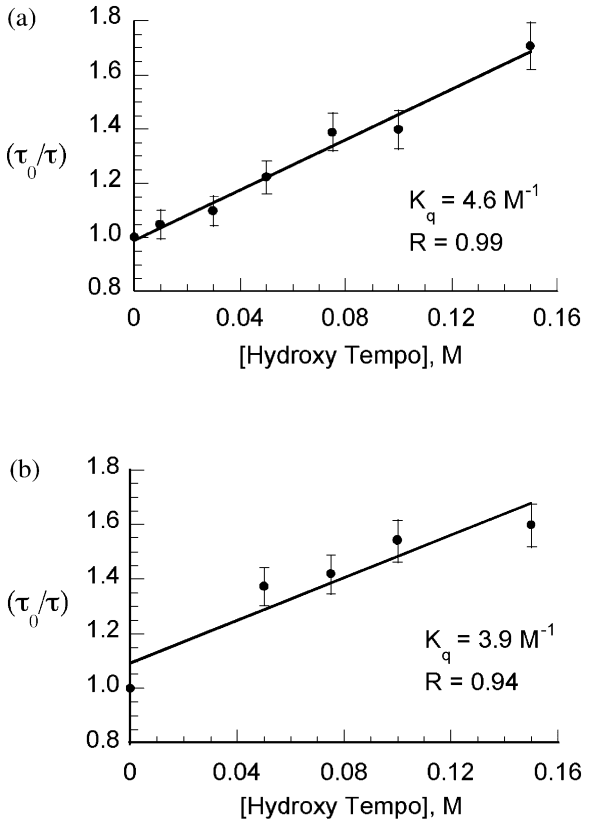

Fig. 6. Stern–Volmer plot for fluorescence quenching of StDNP label by nitroxide radical. (a) Free label; (b) StDNP–antiDNP (monoclonal) complex. Solution: glycerol (50%), PBS buffer (40%), DMSO (10%), experimental conditions: excitation 350 nm, emission 438 nm, 25 °C.

in the amino acid sequence of the variable regions of the different antibodies in this set [47].

3.3.2. Antigen binding site protein dynamics based upon the dynamics of the bound StDNP and NslDNP probes

One can discuss a correlationship between the motion of the bound StDNP label and the intermolecular mobility of the Fab fragment based upon analyses of data originating from various sources. These include the fluorescence–photochrome and nitroxide spin-label motional data noted above together with data on ligand binding thermodynamics. In addition, NMR data for aromatic groups in the binding site's vicinity, plus X-ray crystallographically determined thermal parameters for atoms, coupled with molecular dynamics studies of the protein, and the ligand doping computer molecular graphics simulations reported in our work were also used.

Nanosecond dynamics of the stilbene and nitroxide probes in the antibody binding sites cannot be explained by a fast exchange between bound and free probes. The experimental rate constant for Ns/DNP/antiDNP complex dissociation was found to be $k_d = 500\ s^{-1}$ [48], which is essentially less than the probe's correlation frequency. It has previously been shown [31,45] that in the presence of Fab, three DNP proton signals in the DNPGly hapten are of the order of 50 times broader compared to those from the same nuclei when the molecule is free in solution. The authors explained this broadening in terms of chemical exchange between free and bound label. The exchange obviously occurs in the millisecond temporal range of the NMR time-scale.

Of the heavy (H) and light (L) chains making up the four Fab domains [constant (*C*) domains C_H and C_L at the C-terminal ends, and variable (*V*) domains V_H and V_L], the latter two are important structural units since they form the antigen binding site. The angle between the pseudodyad axis within the two *V* parts and the axis between the two *C* parts has been described as an 'elbow-bend'. According to X-ray structural analysis and electron microscopy data, this angle significantly varies in Fab structures from different sources, and this has been interpreted as indirect evidence in favor of wobbling around these axes ([16,17,30], and references therein). Molecular dynamics simulations of uncomplexed Fab in solution [49] suggest a low-amplitude motion of the protein domains with respect to one another, reflected by a periodic alternation of the elbow-bend angle within a range of 11°. Insertion of the hapten into the binding site changes the elbow-bend angle by almost 30°. Taking in consideration the molecular mass of V_H, V_L, C_H and C_L macromolecular subunits, we can conclude that the correlation time of their low amplitude mutual mobility is equal to, or longer than, 10 ns. This is markedly higher than τ_c for the StDNP and Ns*l*DNP probes in the binding site. The Fab dynamics simulations [49,50] showed that the amplitude of mutual motion of two variable domains does not exceed 1 Å, and, therefore, the probe's motion cannot be realized by a mutual movement of the V_H and V_L domains.

The 2.9 Å resolution X-ray determined structure of the Ns*l*DNP/antiDNP antibody complex [30] provides isotropic thermal parameter ('B'-value) data for an analysis of possible dynamics of various parts of the hapten–antibody complex. B-factors for atoms related by bond angles in main-chains were set to 2.0 $Å^2$, pointing out the rigidity of the chain. An overall B-factor of 15 $Å^2$ was maintained for all atoms. In the antigen binding site region, the average B-parameters for the side-chain atoms of c Trp 91 L and Trp 96 H were reported to be 18.2 and 11.8 $Å^2$. While the electron density for the hapten was also noted to be 'quite good', the isotropic thermal B-parameters, for the hapten were described as being higher than those for neighboring residues [30]. This is readily seen by the 37.4 $Å^2$ average B-values for the hapten-TEMPO ring, while the 22.9 $Å^2$ average B-values for the hapten-DNP ring are slightly higher than the average B-values mentioned above for the tryptophanyl side chain moieties at the binding site. Therefore, on the time-scale of the X-ray crystallographic measurement, the Ns*l*DNP hapten appears to undergo more dynamic motion or static disorder than its surroundings with 'amplitudes' (root square from B) for Trp 91 L, Trp 96 H, DNP and TEMPO groups approximately 4.2, 3.4, 6.1 and 4.8 Å, correspondingly. These 'amplitudes' of

above mentioned groups wobbling are comparable with the group's radius.

The tryptophan moieties are connected with the main-chains by a flexible spacer of two CH_2 groups. Thus, we conclude that wobbling of the rigid binding site/Ns*l*DNP hapten ensemble (Trp 91 L, Trp 96 H, DNP-ring, TEMPO-ring), as well as that for the corresponding StDNP analogue, can be responsible for the label's nanosecond dynamics detected by ESR and fluorescence polarization techniques. This mechanism of Fab dynamics in the vicinity of the binding site appears to be the most probable. The mobility of Trp 91 L and Trp 96 H moieties provides the induced fit for effective stacking and release of the DNP epitope.

4. Conclusion

Protein intramolecular mobility shows a significant dependence upon the molecular dynamics of the immediate solvent medium which provides the free volume for movement of protein domains and individual functional groups. A combined fluorescence–photochrome approach was used for investigation of the state of the medium's microviscosity within the binding site cavity of antiDNP antibodies. The fluorescent DNP analogue, 4-(*N*-2,4-dinitrophenylamino)-4′-(*N*,*N*′-dimethylamino)stilbene label (StDNP), **1**, was incorporated into the binding site followed by measurement of a set of fluorescence and photochrome parameters (such as the StDNP excitation and emission spectra, fluorescence life time, steady-state and time-resolved fluorescence polarization, *trans–cis* and *cis–trans* photoisomerization kinetics, and fluorescence quenching by nitroxide radicals freely diffused in solution). In parallel and independently, computational molecular graphics modeling of the position and dynamics of the StDNP and spin nitroxide-DNP (Ns*l*DNP) labels in an AN02 Fab fragment model of the binding site were also undertaken.

On the basis of the available experimental and computational data we came to the following conclusions.

(1) The StDNP probe undergoes anisotropic rotation in the 6 cP solvent mixture-A solution as a whole molecule with a correlation time $\tau_c = 1.1$ ns. This is much faster than theoretically predicted from the rotation barrier in vacuum about the C–N bond connecting the DNP and stilbene fragments ($\tau_c = 19$ ns).

(2) The StDNP probe in both *trans*- and *cis*-conformation forms a complex with the antibody binding site ($K_d = 1.2 \times 10^{-6}$ M for the *trans*-conformation) in which the DNP fragment is squeezed between two parallel tryptophanyl rings according to the model.

(3) Data on fluorescence polarization of StDNP, and analysis of the ESR spectrum of Ns*l*DNP, indicate that both labels in the binding site are involved in anisotropic rotation with correlation times of 4 and 2.5 ns, respectively. This rotation is significantly faster than the mobility of the antiDNP antibody and Fab fragments and than theoretically calculated rotation about the C–N bond between the DNP moiety and the stilbene and nitroxide fragments in StDNP ($\tau_c = 19$ ns) and in Ns*l*DNP ($\tau_c = 1.5$ s).

(4) The results of the photoisomerization kinetics experiments provide a confirmation of the computer modeling prediction of sufficient space for twisting of the StDNP stilbene fragments in the excited singlet-state without any steric hindrance. The estimated 'microviscosity' parameter, the twisting correlation time ($\tau_c = 1$ ns), is found to be close to the unbound label's anisotropic rotational correlation time in solution ($\tau_c = 1.1$ ns). Therefore, the microviscosity of the medium in the binding site cavity does not differ markedly from the bulk viscosity.

(5) As predicted by computer modeling, the StDNP fluorescence quenching experiments indicate that nitroxide quencher access to the bound stilbene fragment in the complex to afford encounter complexes is limited by an apparent steric factor of approximately 0.5. The viscosity of the binding site cavity in the area of the stilbene label at distance approximately 5 Å from the protein tryptophanyl groups is close to the bulk viscosity.

All the experimental evidence suggests that wobbling of the rigid binding site/Ns*l*DNP hapten ensemble (Trp 91 L, Trp 96 H, DNP-ring, TEMPO-ring), as well as that for the corresponding StDNP analogue, can be responsible for the label's nanosecond dynamics detected by ESR and fluorescence polarization techniques. Thus, this mech-

anism describing the molecular dynamics of the Fab binding site appears to be the most probable. In accord with the experimental findings, the mobility of Trp 91 L and Trp 96 H moieties provides the induced fit needed for effective stacking and release of the DNP epitope. As a result, we have shown that the combined fluorescence–photochrome approach can be used for investigation of local medium molecular dynamics in the immediate vicinity of specific sites of proteins and nucleic acids, as well as for other biologically important structures and synthetic analogues.

Acknowledgments

The authors thank Vladislav Papper for providing the stilbene probe, Dr Natalia Strashnikova and Batia Uzan for technical assistance. We acknowledge with gratitude the valuable advices of Prof. Avraham Parola and Dr Itay Adin. This work was funded by a grant from the German–Israeli James Franck Program on Laser–Matter Interactions, and by the Harry Stern Applied Research Grant Program.

References

[1] R. Lumry, H. Eyring, Conformation change of proteins, J. Phys. Chem. 58 (1954) 110–120.
[2] K.H. Linderstrom-Lang, J.A. Schellman, Protein structure and enzyme activity, in: P.D. Boyer, H. Lardy, K. Myrback (Eds.), The Enzymes, vol. 1, Academic Press, New York, 1959, pp. 443–510.
[3] D.J. Koshland, Mechanism of transfer of enzymes, in: P.D. Boyer, M. Lardy, K. Myrback (Eds.), The Enzymes, vol. 1, Academic Press, New York, 1959, pp. 305–346.
[4] L. Berliner (Ed.), Spin Labeling. Theory and Application, vol. 1, Academic Press, New York, 1976.
[5] L. Berliner (Ed.), Spin Labeling. Theory and Application, vol. 2, Academic Press, New York, 1979.
[6] G.I. Likhtenshtein, Spin Labeling Methods in Molecular Biology, Wiley-Interscience, New York, 1976, pp. 125–148.
[7] G.I. Likhtenshtein, The water–protein interaction and dynamic structure of proteins, in: A. Alfsen, A.J. Bertreaud (Eds.), L'eau les Systems Biologic, Edition CNRS, Paris, 1976, pp. 45–52.
[8] G.I. Likhtenshtein, Biophysical Labeling Methods in Molecular Biology, Cambridge University Press, Cambridge, 1993, pp. 180–195.
[9] G.I. Likhtenshtein, V.R. Bogatyrenko, A.V. Kulikov, Low temperature protein dynamics studied by spin-labelling methods, Appl. Magn. Reson. 4 (1993) 513–521.
[10] R. Lumry, R. Biltonen, in: S.N. Timashev, C.D. Fosman (Eds.), Structure and Stability of Biological Molecules, vol. 2, Marcel Dekker, New York, 1969, pp. 146–306.
[11] G.R. Welch (Ed.), The Fluctuating Enzymes, Wiley, New York, 1986.
[12] G.I. Likhtenshtein, Water and dynamics of proteins and membranes, Studia Biophys. 11 (1986) 89–100.
[13] P.S. Steinbach, R.J. Loncharich, B.R. Brooks, The effect of environment and hydratation on protein dynamics: a simulation study of myoglobin, Chem. Phys. 158 (1991) 383–394.
[14] R.B. Gregory (Ed.), Protein–Solvent Interactions, Marcel Dekker, New York, 1994.
[15] G.I. Likhtenshtein, F. Febbrario, R. Nucci, Intramolecular dynamics and conformational transition in proteins studied by biophysical labeling methods, Spectrochim. Acta 56 (Part A) (2000) 2011–2031.
[16] R. Nezlin, Internal movement in immunoglobin molecules, Adv. Immunoglobin Mol. 48 (1990) 1–40.
[17] R. Nezlin, The Immunoglobins. Structure and Function, Academic Press, San Diego, 1998, pp. 259–261.
[18] Y.P. Sun, J. Saltiel, Application of the Kramers equation to stilbene photoisomerization in *n*-alkanes using translational diffusion coefficients to define microviscosity, J. Phys. Chem. 93 (1989) 8310–8316.
[19] D.H. Waldeck, Photoisomerization dynamics of stilbenes, Chem. Rev. 91 (1991) 415–436.
[20] R. Lapouyade, K. Czeska, W. Majenz, W. Rettig, E. Gilbert, C. Rulliere, Photophysics of donor–acceptor substituted stilbenes, J. Phys. Chem. 96 (1992) 9643–9650.
[21] V. Papper, G.I. Likhtenshtein, Substituted stilbenes: a new view on well-known systems. New application in chemistry and biophysics, Photochem. Photobiol. A: Chem. 140 (2001) 39–52.
[22] V.M. Mekler, G.I. Likhtenshtein, Study of dynamic contacts of macromolecules according to kinetics of isomerization of fluorescent label sensitized by the dye in a triplet state, J. Biophys. 31 (1986) 568–571.
[23] G.I. Likhtenshtein, D.V. Khudjakov, V.R. Vogel, Photochrome-labeling method in the study of dynamics of biological systems, J. Biochem. Biophys. Methods 25 (1992) 219–229.
[24] G.I. Likhtenshtein, Rizak Bishara, V. Papper, et al., Novel fluorescence–photochrome labeling method in the study of biomembrane dynamics, J. Biochem. Biophys. Methods 33 (1996) 117–133.
[25] V. Papper, G.I. Likhtenshtein, D. Pines, E. Pines, Photochemical and photophysical characterization of 4,4′-substituted stilbenes: linear free energy, in: S.G. Pandalai (Ed.), Recent Research Developments in Photochemistry and Photobiology, vol. 1, Transworld Research Network, Trivandrum, India, 1997a.

[26] V. Papper, G.I. Likhtenshtein, D. Pines, E. Pines, Biophysical and biochemical characterization of *para*-substituted stilbenes, Photochem. Photobiol. A: Chem. 111 (1997b) 87–96.

[27] V. Papper, G.I. Likhtenshtein, N. Medvedeva, D.V. Khoudyakov, Quenching of cascade reaction between triplet and photochrome probes with nitroxide radical, Photochem. Photobiol. A: Chem. 122 (1999) 79–85.

[28] N.V. Strashnikova, V. Papper, P. Parchomuck, V. Ratner, G.I. Likhtenshtein, R. Marks, Local medium effect in the photochemical behavior of substituted stilbenes immobilized on quartz surfaces, Photochem. Photobiol. A: Chem. 122 (1999) 133–142.

[29] N. Medvedeva, I. Fishov, G.I. Likhtenshtein, Quenching of cascade reaction between triplet and photochrome probes with nitroxide radicals: novel labeling method in study of membranes and surface system, J. Appl. Biotech. Biophys. 89 (2000) 231–248.

[30] A.T. Brünger, D.J. Leahy, T.R. Hynes, R.O. Fox, 2.9 Ångstrom resolution structure of an anti-dinitrophenyl-spin-label monoclonal antibody Fab fragment with bound hapten, J. Mol. Biol. 221 (1991) 39–256.

[31] J. Anglister, T. Frey, H.M. McConnell, Magnetic resonance of a monoclonal anti-spin-label antibody, Biochem. 23 (1984) 1138–1142.

[32] S.W. Benson, Thermodynamical Kinetics. Methods for the Estimation of the Thermochemical Data and Rate Parameters, Wiley, New York, 1968.

[33] S.J. Temkin, B.J. Jacobson, Diffusion controlled of chemically anisotropic molecules, J. Chem. Phys. 88 (1984) 2679–2685.

[34] G. Weber, Polarization of the fluorescence of macromolecules. 1. Theory and experimental method, Biochem. J. 51 (1952) 145–155.

[35] C. Lovejoy, D.A. Holovka, R.E. Cathou, Nanosecond fluorescence spectroscopy of pyrenbutyrate–antpyren butyrate antibody complexes, Biochemistry 16 (1977) 3668–3671.

[36] D.C. Hanson, J. Yguerabide, V.N. Shumaker, Segmental flexibility of IG antibody molecules in solution: a new interpretation, Biochemistry 20 (1985) 6842–6852.

[37] D. Marsh, Experimental methods in spin-label spectral analysis, in: L.J. Berliner, J. Reubin (Eds.), Spin Labeling. Theory and Applications, Plenum Press, New York, 1989, pp. 255–285.

[38] J.H. Freed, Theory of the ESR spectra of nitroxides, in: L. Berliner (Ed.), Spin Labeling. Theory and Application, vol. 1, Academic Press, New York, 1976, pp. 255–285.

[39] V.I. Krinichnyi, Investigation of biological systems by high resolution 2-mm wave band ESR, J. Biochem. Biophys. Methods 23 (1991) 1–28.

[40] V.I. Krinichnyi, 2-mm Wave Bond ESR Spectroscopy of Condensed Systems, CRC Press, Boca Raton, 1994, pp. 101–119.

[41] V.I. Krinichnyi, O.Ya. Grinberg, V.R. Bogatirenko, G.I. Likhtenshtein, Ya.S. Lebedev, Study of microenvironment effect on magnetic parameters of spin-labeled human serum albumin in the 2-mm ESR range, Biofizika 30 (1985) 216–223.

[42] I.V. Dudich, V.P. Timofeev, M.V. Volkenshtein, A.Yu. Misharin, Measurement of the correlation time of rotational diffusion of macromolecules with covalently bound spin label by ESR method, Mol. Biol. (Moscow) 11 (1977) 685–692.

[43] J.R. Lakowicz, Principles of Fluorescence Spectroscopy, Plenum Press, New York, 1983.

[44] J.R. Little, H.N. Eisen, Evidence for tryptophan in the active sites of antibodies to polynitrobenzenes, Biochemistry 6 (1967) 3119–3125.

[45] J. Anglister, M.W. Bond, T. Frey, et al., Contribution of tryptophan residues to the combining site of a monoclonal anti dinitrophenyl spin-label antibody, Biochemistry 26 (1987) 6058–6064.

[46] R.A. Dwek, S. Wain-Hobson, S. Dower, et al., Structure of an antibody combining site by magnetic resonance, Nature 226 (1977) 31–37.

[47] D.J. Leahy, G.S. Rule, M.M. Whittaker, H.M. McConnell, Sequences of 12 monoclonal anti-dinitrophenyl spin-label antibodies for NMR studies, Proc. Natl. Acad. Sci. USA 85 (1988) 3661–3665.

[48] T.P. Theriault, D.J. Leahy, M. Levitt, M.H. McConnell, Structural and kinetic studies of the Fab fragment of a monoclonal anti-spin label antibody by nuclear magnetic resonance, J. Mol. Biol. 221 (1991) 257–270.

[49] C.A. Sotriffer, K.R. Liedl, D.S. Linthicum, B.M. Rode, J.M. Varga, Ligand-induced domain movement in an antibody Fab: molecular dynamics studies confirm the unique domain movement observed experimentally for Fab NC6.8 upon complexation and reveal its segmental flexibility, J. Mol. Biol. 278 (1998) 301–306.

[50] C.A. Sotriffer, W. Flader, B.M. Rode, K.R. Liedl, J.M. Varga, Automated docking of ligands to antibodies: methods and applications, Methods 20 (2000) 280–291.